Anal Bioanal Chem (2015) 407:7807–7814
DOI 10.1007/s00216-015-8949-y

RESEARCH PAPER

A biosensor based on electroactive dipyrromethene-Cu(II) layer deposited onto gold electrodes for the detection of antibodies against avian influenza virus type H5N1 in hen sera

Urszula Jarocka[1] · Róża Sawicka[2] · Anna Stachyra[2] · Anna Góra-Sochacka[2] · Agnieszka Sirko[2] · Włodzimierz Zagórski-Ostoja[2] · Violetta Sączyńska[3] · Anna Porębska[3] · Wim Dehaen[4] · Jerzy Radecki[1] · Hanna Radecka[1]

Received: 6 May 2015 / Revised: 21 July 2015 / Accepted: 31 July 2015 / Published online: 22 August 2015

Abstract This paper describes the development of a biosensor for the detection of anti-hemagglutinin antibodies against the influenza virus hemagglutinin. The steps of biosensor fabrications are as follows: (i) creation of a mixed layer containing the thiol derivative of dipyrromethene and 4-mercapto-1-butanol, (ii) complexation of Cu(II) ions, (iii) oriented immobilization of the recombinant histidine-tagged hemagglutinin, and (iv) filling free spaces with bovine serum albumin. The interactions between recombinants hemagglutinin from the highly pathogenic avian influenza virus type H5N1 and anti-hemagglutinin H5 monoclonal antibodies were explored with Osteryoung square-wave voltammetry. The biosensor displayed a good detection limit of 2.4 pg/mL, quantification limit of 7.2 pg/mL, and dynamic range from 4.0 to 100.0 pg/mL in buffer. In addition, this analytical device was applied for the detection of antibodies in hen sera from individuals vaccinated and non-vaccinated against the avian influenza virus type H5N1. The limit of detection for the assay was the dilution of sera 1: 7×10^6, which is about 200 times better than the enzyme-linked immunosorbent assay.

Keywords Dipyrromethene-Cu(II) layer · Histidine-tagged antigen immobilization · Detection of antibodies in sera · Avian influenza virus

Introduction

The highly pathogenic avian influenza (HPAI) virus can be easily transmitted among poultry which often leads to severe disease outbreaks or even pandemics. All these cause enormous economic losses in the poultry industry and seriously threaten human health [1–3]. Therefore, methods suitable for early and fast detection of the highly pathogenic forms are still desired.

Among a variety of available analytical techniques, which are currently applied to detection of AI, the biosensors are promising tools. These are generally defined as analytical devices consisting of biological components (e.g., tissues, microorganisms, proteins, enzymes, antibodies, nucleic acids, etc.) coupled to transducers, generating analytical responses related with the analyte concentrations in samples [4, 5]. Biochemical sensors have attracted considerable attention due to selectivity, sensitivity, and possibility of miniaturization. They have found numerous applications for control of food quality, environmental pollution, and medical diagnostics, just to name a few examples [6–8].

In recent years, there has been a growing interest in the development of electrochemical biosensors based on redox active layers immobilized on the electrode surface [9]. Such layers could serve as transducers, as well as sites for stable and oriented immobilization of biological molecules. The redox

Electronic supplementary material The online version of this article (doi:10.1007/s00216-015-8949-y) contains supplementary material, which is available to authorized users.

✉ Hanna Radecka
h.radecka@pan.olsztyn.pl

[1] Institute of Animal Reproduction and Food Research, Polish Academy of Sciences, Tuwima 10, 10-748 Olsztyn, Poland

[2] Institute of Biochemistry and Biophysics, Polish Academy of Sciences, Pawińskiego 5A, 02-106 Warsaw, Poland

[3] Institute of Biotechnology and Antibiotics, Starościńska 5, 02-516 Warsaw, Poland

[4] Department of Chemistry, University of Leuven, Celestijnenlaan 200F, 3001 Leuven, Belgium

centers, located inside the active sensing layers, are responsible for transduction of signals coming from the recognition process to analytically readable signals. The main advantage of the biosensors based on the redox active layers is that there is no need for a redox marker in the sample solution [10].

The properties of the redox active layers mostly depend on the distance from the redox center to the electrode surface, the structure of the bridge connecting the redox active center, and the electrode surface, as well as the molecular environment around the redox center [11].

Controlling the molecular structure, organization, and orientation of proteins on solid surfaces without distressing their function is a key in the development of biosensors. Initially developed for the biochemical purification of genetically engineered proteins, the formation of ternary metal–chelate complexes between nitrilotriacetic acid (NTA) or imminodiacetic acid (IDA) and histidine-tagged (His-tagged) recombinant proteins has shown to be a promising strategy for controlling protein orientation at interfaces, requiring only mild protein modification. Furthermore, this specific immobilization is reversible, which allows the release and recovery of the immobilized protein under mild conditions [12]. Such strategy was successfully applied to the construction of sensors [13–17].

Dipyrromethene derivatives (DPM), which have high affinity towards transition metal ions, are suitable for the formation of the layer with the redox centers by performing the successive complexation reactions on the electrode surface [18]. This system based on a redox active DPM–Cu(II) complex for oriented immobilization of His-tagged proteins was originally introduced and described in our previous work [16, 17]. The binding affinity of His-tagged protein to the dipyrromethene-Cu(II) complex has been confirmed using surface plasmon resonance (SPR) [19]. The DPM-Cu(II) layer incorporated with His_6-protein was stable during several hours. Also, we did not observed any changes of electrochemical parameters recorded in the buffer solution before starting of analyte measurements.

Here, we present the biosensor based on ternary metal–chelate complex between DPM and the recombinant His-tagged hemagglutinin (His_6-H5 HA). The sensor allowed for precise detection of antibodies against hemagglutinin (HA) from the HPAI virus H5N1. A specific interaction between the His_6-H5 HA and the appropriate monoclonal antibody was observed using Osteryoung square-wave voltammetry (OSWV). The biosensor proposed detected specific anti-H5 HA antibodies in buffer solution, as well as in hen sera samples.

Experimental

Chemicals and materials

DPM was synthesized by ProChimia Surfaces Company (Sopot, Poland). 4-Mercapto-1-butanol (MBT), phosphate buffer saline (PBS) components (137 mM NaCl, 2.7 mM KCl, 1.8 mM Na2HPO4, 10 mM KH2PO4), copper (II) acetate, and chloroform were obtained from Sigma-Aldrich (Poznań, Poland). Alumina 0.3 and 0.05 μm were purchased from Buehler (Lake Bluff, IL, USA). Sulphuric acid, potassium hydroxide, and methanol were supplied by POCh (Gliwice, Poland). Bovine serum albumin (BSA) was purchased from Invitrogen Life Technologies (Darmstadt, Germany). Anti-hemagglutinin H5 monoclonal antibodies (Mab 6-9-1) was obtained from the Institute of Biotechnology and Antibiotics (Warsaw, Poland) and monoclonal anti-IL-2 antibodies from AbD Serotec (Oxford, UK). Two different hen sera from vaccinated (serum 1 from a high responder and serum 2 from a low responder) and from non-vaccinated (serum 3) were collected and characterized in the Institute of Biochemistry and Biophysics (Warsaw, Poland). The negative control (serum 4), provided by the National Veterinary Research Institute (Puławy, Poland), was obtained from chickens hatched from the specific pathogen free (SPF) embryonated eggs (VALO-Biomedia, Osterholz-Scharmbeck, Germany). The recombinant HA antigen used in this study was based on the sequence of H5N1 (A/swan/Poland/305-135V08/2006; EpiFlu Database Acc No EPI156789) and produced in a baculovirus system (Oxford Expression Technologies, Oxford, UK). It covers a region of 17–530 residues with deletion of 6 residues in the proteolytic cleavage site (RRRKKR; 341–346) and contains a His-tag at the C-terminus.

All aqueous solutions were prepared using Milli-Q water, with resistivity 18.2 MΩ·cm (Millipore, Darmstadt, Germany). Reagents and solvents were of analytical grade and used without further purification. Experiments were carried out at room temperature unless stated otherwise.

Preparation of the biosensor

Gold disc electrodes (2 mm diameter) were obtained from Bioanalytical System (BAS, West Lafayette, IN, USA). These electrodes, after washing with methanol (caution: methanol is highly flammable and toxic) and Milli-Q water, were polished in alumina slurries (Alpha and Gamma Micropolish, Buehler, Lake Bluff, IL, USA) with particles size of 0.3 and 0.05 μm on microcloth polishing pads for 5 min each. Afterwards, they were carefully washed with Milli-Q water. Then, electrochemical cleaning was performed by cyclic voltammetry (CV). The gold electrodes were cleaned electrochemically with using the silver chloride reference electrode (Ag/AgCl) and the platinum wire counter electrode in 0.5 M potassium hydroxide solution and next in 0.5 M sulphuric acid solution. In the first step, in 0.5 M potassium hydroxide solution, the potential was swept with a scan rate of 0.1 V/s between −0.4 and

−1.2 V. The gold electrodes were first submitted to 3 cycles, then to 50 additional cycles, and finally to 10 more cycles. All of them have been performed under the same condition. Next, the electrodes were cleaned in 0.5 M sulphuric acid solution. The potential was swept with a scan rate of 0.1 V/s between −0.3 and +1.5 V. Initially, they have been submitted to 3 cycles, then to 10 cycles, and finally to 3 more cycles performing under the same conditions. After finishing the electrochemical cleaning, each electrode was rinsed with Mili-Q water and stored in water (for several minutes, until the next step) to avoid contamination from air. All solutions were deoxygenated by purging with nitrogen (ultra pure 6.0, Air Products, Warsaw, Poland) for 10 min.

Directly after cleaning, the electrodes were washed repeatedly with Milli-Q water and methanol. Subsequently, they were soaked in a mixed solution of 0.01 mM DPM and 1 mM MBT in chloroform (caution: chloroform is toxic and a suspected carcinogen) for 3 h. Next, after washing with chloroform and chloroform/methanol solution (1:1), the electrodes were dipped in 1 mM Cu(II) acetate solution in chloroform/methanol (1:1) for 1 h. The tubes containing electrodes were sealed with Teflon tape to avoid solvent evaporation. Then, after washing with chloroform/methanol (1:1) solution, methanol, water, and PBS buffer, the electrodes were fixed upside down and a 10 μL of 1 μg/mL His_6-HA H5 (in 0.1 M PBS, pH 7.4) were placed on the gold surfaces for 1 h. BSA solution in a concentration of 1 % (*m*/*v*) was used for blocking any unspecific binding. As in earlier steps, 10-μL droplets were applied on the surface of each electrode and left for 30 min. Finally, the electrodes were rinsed with 0.1 M PBS. Fully modified electrodes were stored in a refrigerator (+4 °C) in 0.1 M PBS, pH 7.4 until used, but not longer than 1 day.

A specific interaction between the His_6-H5 HA and antibodies

Mab 6-9-1 and anti-IL-2 antibodies were diluted in the buffer (0.1 M PBS, pH 7.4) to the concentration of 0, 4, 25, 50, 75, and 100 pg/mL. The samples of the hen sera from: the vaccinated (serum 1 from a high responder and serum 2 from a low responder), non-vaccinated (serum 3) and chickens serum hatched from the specific pathogen free (serum 4) were prepared in the PBS buffer (10-fold serial dilutions in the range from 1:7×102 to 1:7×108). The reactions between the His_6-H5 HA and antibodies were performed by dropping of the 10-μL aliquots of the respective dilutions of the analytes on the Au–MBT/DPM–Cu(II)–His6-H5HA–BSA modified electrode surfaces. The electrodes were covered by Eppendorf tubes in order to protect against evaporation and air pollution. After 0.5 h of incubation at room temperature, the electrodes were rinsed with 5 mL of 0.1 M PBS, pH 7.4 in order to remove the unbound analytes.

Osteryoung square-wave voltammetry measurements

Electrochemical measurements were performed with an Autolab potentiostat-galvanostat (Eco Chemie, Utrecht, Netherlands). A three-electrode configuration was applied: the gold electrode as a working electrode and a Ag/AgCl reference electrode and a Pt counter electrode. OSWV was performed with potential from 0.55 to −0.25 V with a square wave frequency of 25 Hz and amplitude of 0.05 V.

Results and discussion

Fabrication of the biosensor—successive steps of gold electrode modification

The process of the biosensor formation is shown in Scheme 1. First, a mixed DPM and MBT layer in molar ratio 1:100 was created on the gold electrode surface. Then, Cu(II) ions were complexed by DPM. The Cu(II) ions played the roles of electroactive centers. MBT was applied as spacer molecule in order to prevent unspecific adsorption of Cu(II) ions and intramolecular interactions between the redox centers. The presence of Cu(II) ions on the gold electrode surface was verified using CV performed at different scan rates. Representative cyclovoltammograms are presented in Fig. S1 (see Electronic Supplementary Material, ESM). The reduction of Cu(II) ions and oxidation of Cu(I) ions were observed at E_{pc}=0.290 V and E_{pa}=0.377 V, respectively, at the scan rate of 0.1 V/s. The peak separation ΔE_p=0.087 V indicates that the reversibility of the process is quite good. The linear relationship of the anodic and cathodic peaks current versus the scan rates from 0.01 up to 1 V/s pointed out that the redox processes were not diffusion dependent and confirmed the presence of the DPM-Cu(II) complex on the gold electrode surface.

Next, the His_6-H5 HA was immobilized via coordination bonds between the chelated Cu(II) ions and the nitrogen atoms of the His_6-H5 HA. BSA was used to block any remaining free spaces on the gold electrode surface in order to eliminate unspecific binding. The immobilization of the His_6-H5 HA and BSA was monitored by CV (see ESM Fig. S2) and OSWV (see ESM Fig. S3). The CV curves showed a decrease of the Cu(II) redox processes reversibility. In comparison to the CV, the OSWV, which eliminates the capacitive current, was found to be a more suitable technique. The immobilization of the His_6-H5

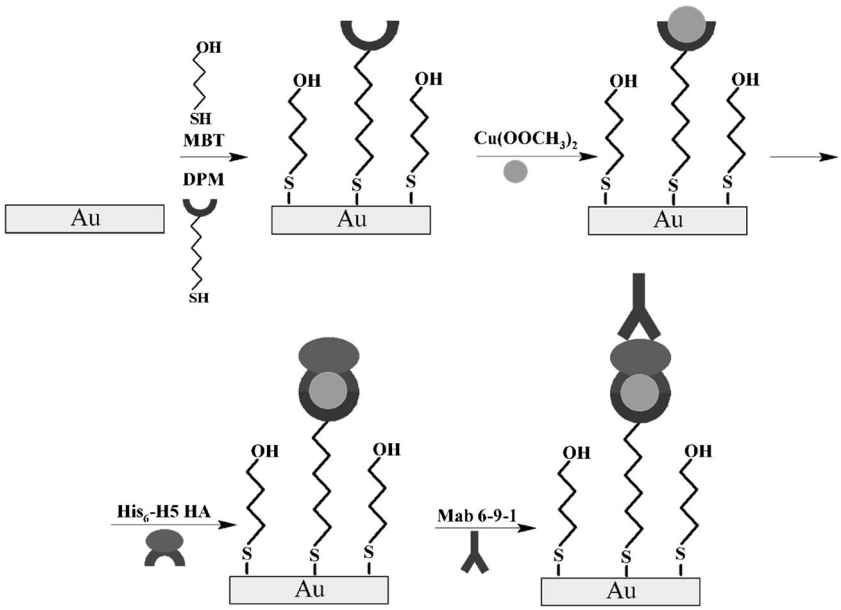

Scheme 1 Steps of biosensor formation

HA and BSA caused a decrease of the Cu(II) peaks current about 75.8 and 66.8 %, respectively.

Detection of the Mab 6-9-1 monoclonal antibodies in buffer

Quantitative assessment of the sensitivity of the biosensor based on the redox active DPM–Cu(II) layer was done with serial dilutions of Mab 6-9-1 in PBS buffer. Typical responses of the biosensor in PBS buffer registered using OSWV are shown in Fig. 1. The Cu(II) ions redox current decreasing is observed with an increasing of the antibodies concentration (Fig. 1A). The negative control (anti-IL-2 antibodies) generated a weak response, what confirmed the selectivity of the biosensor proposed (Fig. 1B).

The biosensor proposed was selective and sensitive. Figure 2 shows the relationships of $(I_n–I_0)/I_0$ [%] vs. concentration c [pg/mL] of Mab 6-9-1 and Mab 6-9-1 in the presence of a constant concentration of anti-IL-2 antibodies (50.0 pg/mL) and anti-IL-2 antibodies in the 0.1 M PBS buffer, pH 7.4. The error bars in the graph stand for standard deviation for 5 or 6 electrodes. The highest concentration (100.0 pg/mL) of Mab 6-9-1 caused significant decreasing of Cu(II) ions redox peak current to 51.6±2.2 % (variability range on sensor-to-sensor was 6.4 %). A linear range of analytical response was observed between 4.0 and 100.0 pg/mL. The limit of detection (LOD) and the limit of quantification (LOQ) were calculated using the equations: LOD=3.3 σ/S and LOQ=10 σ/S (where σ is the standard deviation of the response and S is the slope of the calibration curve) [20]. The LOD and LOQ values were 2.4 and 7.2 pg/mL, respectively. The negative control (anti-IL-2 antibodies), with no affinity to the His_6-H5 HA antigen, generated negligible response. In the presence of the highest concentration (100.0 pg/mL) of anti-IL-2 was observed only a 11.1±4.2 % decrease of the Cu(II) ions redox peak current (Fig. 2).

To check in details the potential cross-reactivity with other antibodies, the OSWV measurements were performed for a series of Mab 6-9-1 dilutions in PBS buffer in the presence of a constant concentration of the anti-IL-2 antibodies (Fig. 1C). The presence of 50.0 pg/mL of anti-IL-2 antibodies only slightly reduces the response of the biosensor towards Mab 6-9-1. The highest concentration of Mab 6-9-1 in the presence of 50.0 pg/mL of anti-IL-2 antibodies generated decreasing of the peak current 44.9±2.1 % (variability range on sensor-to-sensor was 5.5 %) (Fig. 2). The obtained LOD and LOQ values were 4.9 and 14.9 pg/mL, respectively. Thus, it can be concluded that the selectivity of the biosensor proposed based on redox active DPM–Cu(II) layer is sufficient for the detection of Mab 6-9-1.

Detection of the anti-hemagglutinin antibodies in hen sera

Successful calibration against the Mab 6-9-1 suggested that the biosensor could be used for detection of humoral response in biological samples. A series of dilutions of the hen sera from: the vaccinated (serum 1 from a high responder and serum 2 from a low responder), non-vaccinated (serum 3), and chickens serum hatched from the specific pathogen free (serum 4) were prepared in PBS buffer. The sera vaccinated and non-vaccinated hens were selected from the samples of blood collected previously from two groups of chickens immunized with a DNA vaccine based on the H5 HA from the H5N1 (A/swan/Poland/305-135V08/2006) strain of HPAI virus and the control group immunized with the empty vector, respectively [21]. The representative square-wave

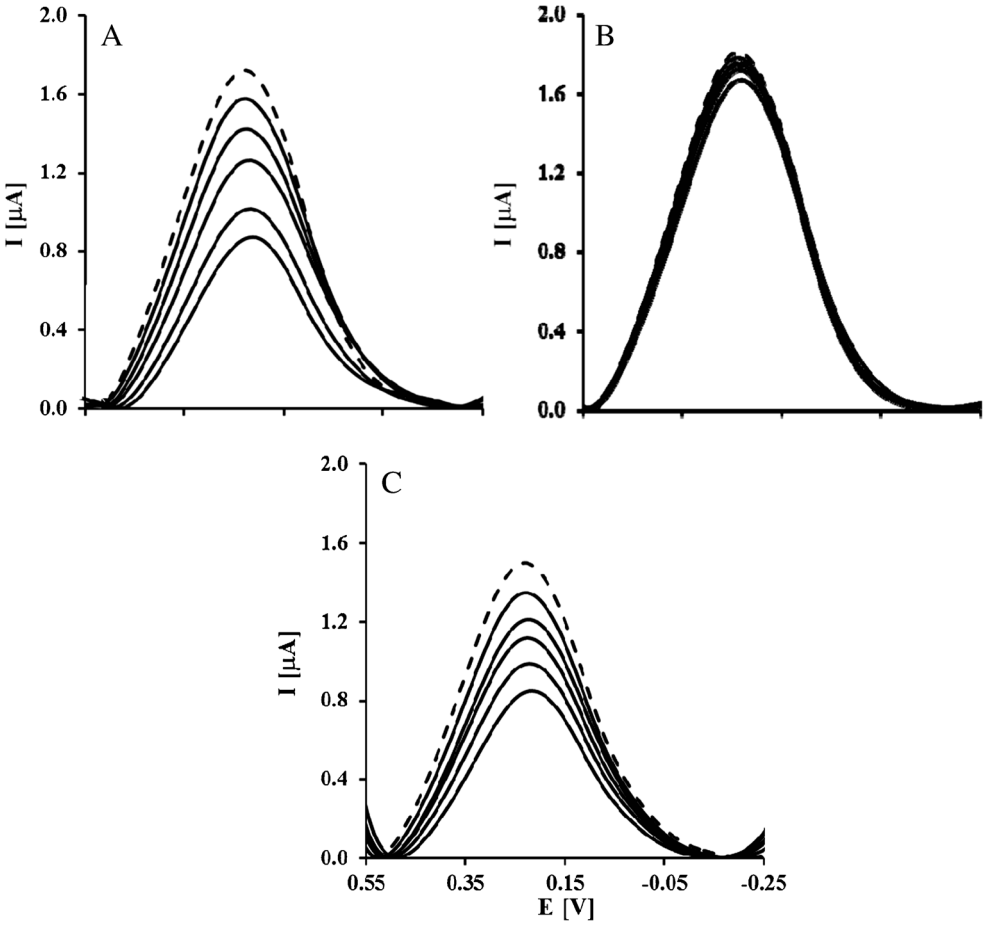

Fig. 1 Typical square wave voltammograms obtained for electrodes modified with Au–MBT/DPM–Cu(II)–His_6-H5 HA–BSA. *Dashed curves* were registered after modification and the following curves after interaction with antibodies: **A** Mab 6-9-1, **B** anti-IL-2 antibodies, **C** Mab 6-9-1 in the presence of a constant concentration of anti-IL-2 antibodies (50.0 pg/mL). Measurement conditions: the Mab-6-9-1 and anti-IL-2 antibodies concentrations: 0, 4, 25, 50, 75, and 100 pg/mL, 0.1 M PBS pH 7.4, square-wave frequency of 25 Hz, and amplitude of 0.05 V

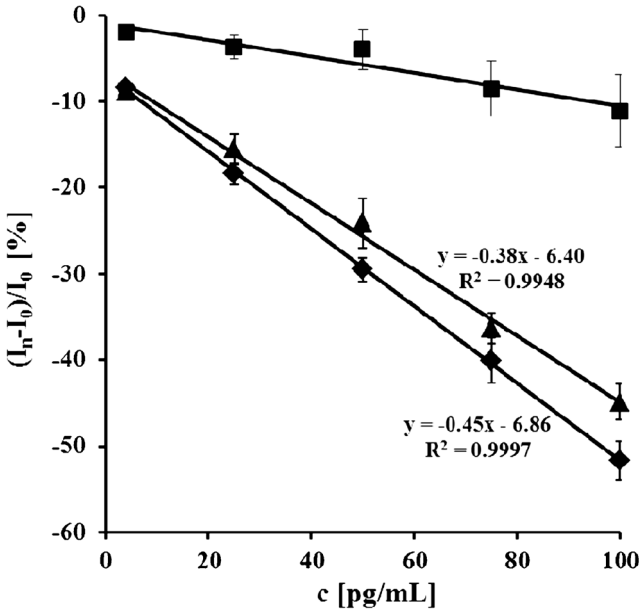

Fig. 2 The relationship of $(I_n–I_0)/I_0$ [%] vs. concentration c [pg/mL] of (*diamond*) Mab 6-9-1 (average from 6 electrodes), (*triangle*) Mab 6-9-1 in the presence of a constant concentration of anti-IL-2 antibodies (50.0 pg/mL) (average from 5 electrodes), (*square*) anti-IL-2 antibodies (average from 5 electrodes) in the presence of 0.1 M PBS pH 7.4

voltammograms are presented in Fig. 3. Upon increasing the contents of antibodies in serum 1, a decrease of the Cu(II) ions redox peaks current was observed (Fig. 3A). A negligible biosensor response was observed in the presence of diluted serum 4 (Fig. 3B).

Figure 4 shows the relationships of $(I_n–I_0)/I_0$ [%] vs. dilutions of different sera. The error bars in the graph stand for standard deviation for 5 or 8 electrodes. The dilution series correspond to increasing concentrations incubated one after the other on a single electrode. The dilution of $1:7\times10^2$ generated decreasing of the peak current 42.5±2.8 % (variability range on sensor-to-sensor was 6.0 %) and 38.2±1.7 % (variability range on sensor-to-sensor was 3.9 %) for serum 1 and serum 2, respectively. The sensor was able to detect anti-H5 HA antibodies in serum 1 diluted $1:7\times10^6$ and serum 2 diluted $1:7\times10^4$. Whereas the lowest dilutions of serum 1 and serum 2 enabling detection of these antibodies by the enzyme-linked immunosorbent assay (ELISA) were $1:2.5\times10^4$ and $1:3\times10^3$, respectively (see ESM Fig. S4). These results indicate that the sensitivity of our biosensor is nearly 200 and 20 times better than ELISA for serum 1 and serum 2, respectively. The slight decrease of peak current in the case of serum 3 (obtained from non-vaccinated hens) could be caused by the matrix (different antibodies, expected to be present in serum 3, could be

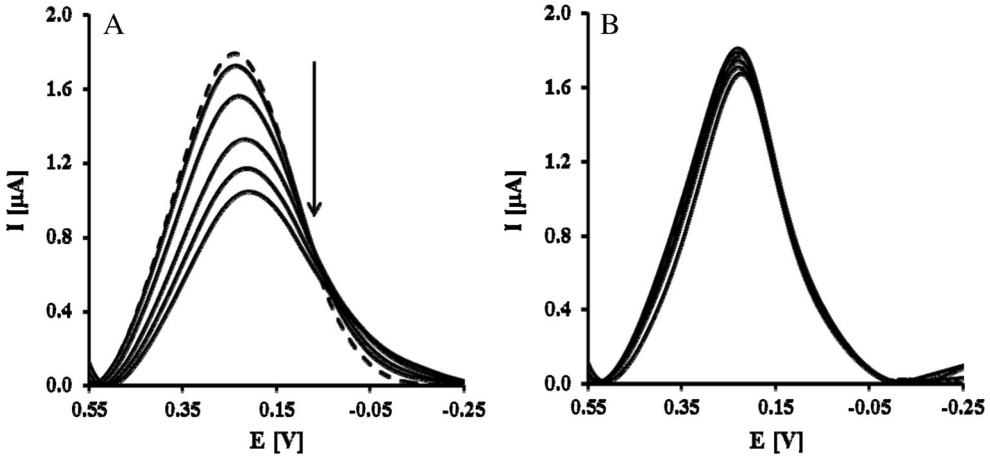

Fig. 3 Typical square wave voltammograms obtained for electrodes modified with Au–MBT/DPM–Cu(II)–His_6-H5 HA–BSA. *Dashed curves* were registered after modification and the following curves after interaction with antibodies in: **A** serum 1 from a high responder, **B** serum 4 (pathogen free). Measurement conditions: 10-fold serial dilutions in the range from 7×10^2 to 7×10^8; 0.1 M PBS pH 7.4; square wave frequency of 25 Hz and amplitude of 0.05 V

generated by hens contact with an environment) of the hen sera. On the other hands, in the presence of serum 4 (totally free from any antibodies), weak responses were observed (Fig. 4). In the presence of the $1:7\times10^2$ dilution of serum 4 was observed only a 8.7±2.0 % decrease of the Cu(II) ions redox peak current.

In our previous paper [22], we have described an impedimetric immunosensor for the detection of anti-H5 HA antibodies. Its preparation consisted of successive modification steps of glassy carbon electrodes: (i) creation of COOH groups, (ii) covalent immobilization of protein A with the EDC/NHS coupling reaction, (iii) covering with anti-His IgG monoclonal antibodies, (iv) immobilization of the His_6-H5 HA, and (v) filling any free space with BSA. The

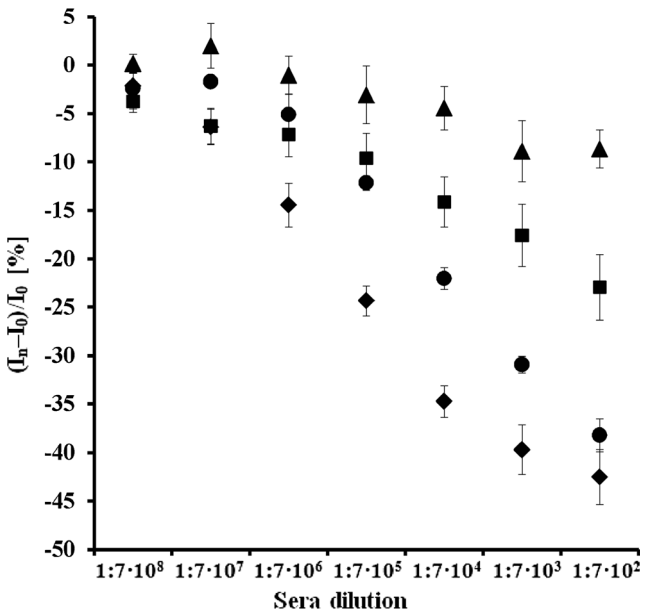

Fig. 4 The relationship of $(I_n–I_0)/I_0$ [%] vs. dilutions of: (*diamond*) serum 1 from a high responder (average from 8 electrodes); (*circle*) serum 2 from a low responder (average from 5 electrodes); (*square*) serum 3 from non-vaccinated (average from 5 electrodes); (*triangle*) serum 4 (pathogen free) (average from 5 electrodes)

interactions between the His_6-H5 HA and anti-H5 HA antibodies have been explored with electrochemical impedance spectroscopy (EIS) in the presence of $[Fe(CN)_6]^{3-/4-}$ as an electroactive marker. The impedimetric immunosensor displayed a good LOD of 2.1 pg/mL in buffer. In addition, it was possible to detect antibodies in hen serum diluted up to 7×10^7-fold. The biosensor presented in this paper has a similar sensitivity in buffer. The main advantage of the proposed device is that DPM–Cu(II) complex served as transducers, as well as sites for stable and oriented immobilization of the His_6-H5 HA on the gold electrode surface. The redox centers, located inside the active sensing layers, are responsible for transduction of signals coming from the recognition process to analytically readable signals. Lack of the need of a redox marker in the sample solution could enable our biosensor application in research field in the future. The miniaturization of this device is under study in our laboratory.

The mechanism of the signal generation by the device proposed is similar to the working principle of biosensor based on His-tagged protein recognition elements immobilized onto the redox-active layers presented in our previous papers [16, 17]. The DPM-Cu(II) redox centers are submerged into the sensing layers deposited on the surface of gold electrode. They play double role: as a binding sites for immobilization of the recombinant histidine-tagged hemagglutinin as well as redox active sites responsible for the analytical signal generation. The binding of anti-HA antibodies caused the change of the His_6-H5 HA conformation. In addition, the permeability of layer deposited on the electrode surface decreased. As a consequence, the counter ions accessibility to the Cu(II) redox centers decreased. Therefore, the balance of the charge occurred on the redox centers upon oxidation/reduction processes become more difficult causing the hindering the electron transfer. As the results, upon binding of anti-HA antibodies, a decrease of the Cu(II) ions redox current was observed (Figs. 1 and 3). The similar phenomenon was reported by Stobiecka and Hepel [23].

Table 1 Comparison of the immunosensor presented with those already published

Analyte	Measuring technique	Detection limit in buffer [pg/L]	Determination in real samples	References
Anti-HA	EIS	1	Not determined	[24]
IgG	EIS	570	0.181 mg/mL in CSF	[25]
Anti-F. tularensis	Amperometry	15,000	165 ng/mL in serum	[26]
Mab 6-9-1	EIS	2.1	$1:7\times10^7$ diluted hen serum	[22]
Anti-tTG	QCM	Not determined	1.3 μg/mL in HS	[27]
Anti-HIV-1	ECL	Not determined	$1:6\times10^4$ diluted HS	[28]
IgG	DPV	4	$1:2\times10^4$ diluted HS	[29]
IgE	OSWV	6300	Not determined	[30]
Anti-measles	EIS	10^6	$1:5\times10^3$ diluted HS	[31]
Anti-L. infantum	SPR	Not determined	$1:6.4\times10^3$ diluted canine serum	[32]
Mab 10B2	SPR	$5\cdot10^6$	Not determined	[33]
H5 HA (Qinghai)	EIS	2.2	Not determined	[34]
Mab 6-9-1	OSWV	2.4	$1:7\times10^6$ diluted hen serum	This work

IgG human immunoglobulin G, *CSF* cerebrospinal fluid, *anti-F. tularensis* antibodies against *Francisella tularensis*, *anti-tTG* anti-tissue transglutaminase antibodies, *QCM* quartz crystal microbalance, *anti-HIV-1* human immunodeficiency virus type 1 antibodies, *ECL* electrochemiluminescence, *HS* human serum, *DPV* differential pulse voltammetry, *IgE* human immunoglobulin E, *anti-L. infantum* anti-*Leishmania infantum* antibodies, *SPR* surface plasmon resonance, *Mab 10B2* monoclonal antibodies against bacterium *Acidovorax avenae* subspecies *citrulli*

They stated that the charge redistribution was responsible for signal transduction in label-free electrochemical glutathione immunodetection.

In Table 1, articles reporting about immunosensors for detection of different antibodies in buffer and real samples have been collected in order to compare their sensitivity with sensitivity of biosensor presented. Taking into account the parameters such as the device sensitivity and selectivity, as well as suitability for analyte determination in real samples, the biosensor presented is superior to immunosensors already reported (Table 1). It is worth to emphasize that the main advantages of the device proposed here are its simple fabrication, with the miniaturization possibility, demanding of small sample volume and the suitability for determination of the antibodies directly in hen sera.

Conclusions

An electrochemically active DPM–Cu(II) complex fulfilled dual role in biosensor development: firstly, as a molecular connector allowed for oriented immobilization of the His_6-H5 HA on the gold electrode surface, and secondly was a transducer of the recognition process between the His_6-H5 HA and the antibodies. The device proposed showed the low LOD and LOQ equal to 2.4 and 7.2 pg/mL in buffer, respectively. The monoclonal anti-IL-2 antibodies, used as a negative control (unspecific to the His_6-H5 HA), generated weak response. The system presented detected specific antibodies in a selective way. In addition, this biosensor was able to detect a humoral response in the sera of hens immunized with DNA vaccine based on the sequence of HA from the H5N1. The limits of detection in serum 1 and serum 2 were $1:7\times10^6$ and $1:7\times10^4$, respectively. Its sensitivity is about 200 to 20 times better than ELISA. Therefore, the high sensitivity and selectivity of the system presented allowed distinguishing hens vaccinated from non-vaccinated ones against AI virus. Consequently, it could be very effective in detection of antibodies for immune surveillance and monitoring of the efficiency of poultry vaccination programs.

Acknowledgments The authors are grateful to Violetta Cecuda-Adamczewska and Grażyna Płucienniczak from Institute of Biotechnology and Antibiotics (Warsaw, Poland) for the hybridoma culture producing Mab 6-9-1. This work was supported by the National Centre for Research and Development (NCBiR) under grant no. PBS2/A7/14/2014, grant no. 679/N-BELGIA/2010/0, COST Action CM10005 "Supramolecular Chemistry in Water" and Institute of Animal Reproduction and Food Research, Polish Academy of Sciences, Olsztyn, Poland. Wim Dehaen thanks the University of Leuven, the FWO-Vlaanderen, and the Ministerie voor Wetenschapsbeleid for financial support.

References

1. Boon ACM, French AMF, Fleming DM, Zambon MC (2001) J Med Virol 65:163–170
2. Santana WI, Williams TL, Winne EK, Pirkle JL, Barr JR (2014) Anal Chem 86:4088–4095
3. Dhumpa R, Handberg KJ, Jørgensen PH, Yi S, Wolff A, Bang DD (2011) Diagn Microbiol Infect Dis 69:258–265
4. Gopinath SCB, Tang T-H, Citartan M, Chen Y, Lakshmipriya T (2014) Biosens Bioelectron 57:292–302

5. Pohanka M, Skládal P (2008) J Appl Biomed 6:57–64
6. Jung S-H, Jang H, Lim M-C, Kim J-H, Shin K-S, Kim SM, Kim H-Y, Kim Y-R, Jeon T-J (2015) Anal Chem 87:2072–2078
7. Chen J, Zhou S, Wen J (2014) Anal Chem 86:3108–3114
8. Pienno PAE, Krull UJ (2005) Anal Bioanal Chem 381:10004–11011
9. Moore KE, Flavel BS, Yu J, Abell AA, Shapte JG (2013) Electrochim Acta 89:206–211
10. Hepel M, Zhong C-J (2012) Functional nanoparticles for bioanalysis, nanomedicine, and bioelectronic devices. ACS Symp Ser 1:293–312
11. Eckermann AL, Feld DJ, Shaw JA, Meade TJ (2010) Coord Chem Rev 254:1769–1802
12. Balland V, Hureau C, Chusano AM, Liu Y, Tron T, Limoges B (2008) Chem Eur J 14:7186–7192
13. Johnson DL, Martin LL (2005) J Am Chem Soc 127:2018–2019
14. Mayer D, Ataka KF, Knoll W, Naumann R, Haber-Pohlmeier S, Richter B, Heberle J (2004) J Am Chem Soc 126:16199–16206
15. Ataka K, Giess F, Knoll W, Naumann R, Haber-Pohlmeier S, Richter B, Heberle J (2004) J Am Chem Soc 126:16199–16206
16. Mikuła E, Wysłouch-Cieszyńska A, Zhukova L, Puchalska M, Verwilst P, Dehaen W, Radecki J, Radecka H (2014) Sensors 14: 10650–10663
17. Jargiło A, Grabowska I, Radecka H, Sulima M, Marszałek I, Wysłouch-Cieszyńska A, Dehaen W, Radecki J (2013) Electroanalysis 25:1185–1193
18. Szymańska I, Orlewska CZ, Janssen D, Dehaen W, Radecka H (2008) Electrochim Acta 53:7932–7940
19. Kurzątkowska K, Mielecki M, Grzelak K, Verwilst P, Dehaen W, Radecki J, Radecka H (2014) Talanta 130:336–341
20. Swartz ME, Krull IS (2012) Handbook of analytical validation, CRC Press Taylor & Francis Group
21. Stachyra A, Góra-Sochacka A, Sawicka R, Florys A, Sączyńska V, Olszewska M, Pikuła A, Śmietanka K, Minta Z, Szewczyk B, Zagórski W, Sirko A (2014) Trials Vaccinol 3:40–49
22. Jarocka U, Sawicka R, Góra-Sochacka A, Sirko A, Zagórski-Ostoja W, Radecki J, Radecka H (2014) Biosens Bioelectron 55:301–306
23. Stobiecka M, Hepel M (2011) Biosens Bioelectron 26:3524–3530
24. Arya SK, Kongsuphol P, Wong CC, Polla LJ, Park MK (2014) Sensors Actuators B 194:127–133
25. Derkus B, Emregul KC, Mazi H, Emregul E, Yumak T, Sinag A (2014) Bioprocess Biosyst Eng 37:965–976
26. Dulay SB, Julich S, Tomaso H, O'Sullivan CK (2014) Anal Bioanal Chem 406:4685–4690
27. Manfredia A, Mattarozzia M, Giannettoa M, Careri M (2014) Sensors Actuators B 201:300–307
28. Zhou J, Gan N, Li T, Hu F, Li X, Wang L, Zheng L (2014) Biosens Bioelectron 54:199–206
29. Cao X, Liu S, Feng Q, Wang N (2013) Biosens Bioelectron 49: 256–262
30. Song W, Li H, Liu H, Wu Z, Qiang W, Xu D (2013) Electrochem Commun 31:16–19
31. Mashazi P, Tetyana P, Vilakazi S, Nyokong T (2013) Biosens Bioelectron 49:32–38
32. Souto DEP, Silva JV, Martins HR, Reis AB, Luz RCS, Kubota LT, Damos FS (2013) Biosens Bioelectron 46:22–29
33. Puttharugsa C, Wangkam T, Houngkamhang N, Yodmongkol S, Gajanandana O, Himananto O, Sutapun B, Amarit R, Somboonkaew A, Srikhirin T (2013) Curr Appl Phys 13:1008–1013
34. Jarocka U, Sawicka R, Góra-Sochacka A, Sirko A, Zagórski-Ostoja W, Radecki J, Radecka H (2014) Sensors 14:15714–15728